DALTON
FULL PAPER

A study of the molecular and electronic structures of the indium(I) phospholyls [In(η^5-$P_2C_3Bu^t_3$)] and [In(η^5-$P_3C_2Bu^t_2$)] by X-ray diffraction, photoelectron spectroscopy and density functional theory †

Guy K. B. Clentsmith,[a] F. Geoffrey N. Cloke,*[a] Matthew D. Francis,[a] Jennifer C. Green,*[b] Peter B. Hitchcock,[a] John F. Nixon,*[a] James L. Suter[b] and David M. Vickers[a]

[a] *School of Chemistry, Physics and Environmental Sciences, University of Sussex, Falmer, Brighton, UK BN1 9QJ. E-mail: j.nixon@sussex.ac.uk*
[b] *Inorganic Chemistry Laboratory, South Parks Road, Oxford, UK OX1 3QR. E-mail: jennifer.green@chem.ox.ac.uk*

Received 6th March 2000, Accepted 6th April 2000
Published on the Web 12th May 2000

The crystal and molecular structures of [In(η^5-$P_2C_3Bu^t_3$)] are reported. He I and He II photoelectron (PE) spectra of [In(η^5-$P_3C_2Bu^t_2$)] and of [In(η^5-$P_2C_3Bu^t_3$)] are assigned by comparison with related systems and with the aid of density functional calculations of the ionisation energies (IE). In both cases the first PE band comprises ionisation from the ring π levels together with an ionisation from a Pσ orbital. The second band is due to ionisation from an In-ring antibonding orbital with In s character. Other Pσ ionisation bands lie at higher IE. Substitution of CBu^t by P within the five membered aromatic ring increases the IE of related bands. Geometry optimisation of the parent complexes [In(η^5-$P_3C_2H_2$)] and [In(η^5-$P_2C_3H_3$)] gave structural parameters in good agreement with the X-ray data. Attempts to find an energy minimum corresponding to η^1-coordination were unsuccessful, the structures reverting to the η^5-coordination mode. Bonding of the ring is principally due to overlap of the two upper occupied π orbitals with the In 5p orbitals. Some rehybridisation at the P atoms assists this overlap. Mulliken population analysis shows the In 5p occupation to be *ca.* half an electron in both cases.

Introduction

Currently there is great interest in the organometallic chemistry of compounds containing monovalent Group 13 elements.[1] This has been fuelled in part by developments in the formation of III–V semiconducting films and devices, for example utilising indium phosphide. Much current research explores the potential of precursors that contain both of the elements of the desired semiconductor in the same molecule.[2] Examples are the recently synthesised[3] thermally stable In(I) complexes [In(η^5-$P_3C_2Bu^t_2$)] **1** and [In(η^5-$P_2C_3Bu^t_3$)] **2**. Compound **1** was shown by X-ray diffraction to have a half sandwich structure, similar to the classic example of subvalent main group chemistry, [In(η-C_5H_5)].[4–7] These complexes are volatile, and are potential single sources for chemical vapour deposition (CVD) of III–V semiconductors.

The organometallic chemistry of $[P_2C_3Bu^t_3]^-$ and $[P_3C_2Bu^t_2]^-$ with d- and f-block metals has been extensively studied but complexes involving polyphospholyl anions combined with main group elements are relatively rare.[8,9] Previous attempts to isolate indium combined with phospholyl ligands to form [In(η^5-PC_4Me_4)] were unsuccessful, with the desired In(I) complex being unstable under the reaction conditions, probably decomposing in a similar way to [In(η^5-C_5Me_5)] in donor solvents.[10] The steric hindrance provided by the *tert*-butyl groups on the carbon atoms tends to promote η^5-coordination over η^1-ligation.[11] Low Lewis basicity was reported for **1** because of the lack of adduct formation when treated with Lewis acids and this effect was suggested to be electronic rather than steric in origin since other In(I) complexes involving bulky ligands are potent bases.[3]

This work examines the electronic structure of [In(η^5-$P_3C_2Bu^t_2$)] and [In(η^5-$P_2C_3Bu^t_3$)] by utilising photoelectron spectroscopy and density functional calculations. Calculations are also carried out on [In(η^5-C_5H_5)] accounting for the bonding present in the half sandwich structure and providing a comparison with the phospholyl ring equivalents. The study elucidates the key factors leading to the η^5 co-ordination, the effect of the phosphorus atoms and the low basicity of **1**.

Experimental

[In(η^5-$P_3C_2Bu^t_2$)] was made by the literature procedure[3] and was purified by sublimation.

Synthesis of [In(η^5-$P_2C_3Bu^t_3$)]

InI (200 mg, 0.83 mmol) and $KP_2C_3Bu^t_3$ (250 mg, 0.82 mmol) were stirred in toluene (40 ml) in an ampoule. The ampoule was evacuated and heated to 110 °C for 24 h. The resulting suspension was filtered and volatiles removed *in vacuo*. Sublimation of the residue yielded [In(η^5-$P_2C_3Bu^t_3$)] (140 mg, 45%) as a pale yellow solid. NMR (C_6D_6): $^{31}P\{^1H\}$ δ 182; ^1H δ 1.31 (s, 9H, Bu^t), 1.47 (s, 18H, Bu^t); MS (EI) 384 (M^+, 33%), 115 (In^+, 100%); Microanalysis, Found (Calc.) C 46.94% (46.90%), H 7.08% (7.08%).

Crystallography

Single crystals of [In(η^5-$P_2C_3Bu^t_3$)] (thin plates) were obtained by slow sublimation *in vacuo*. Data collection was on a CAD4

† Electronic supplementary information (ESI) available: colour versions of Figs. 6, 7 and 8. See http://www.rsc.org/suppdata/dt/b0/b001793k/

diffractometer, The structure solution (direct methods) and refinement were carried out with SHELXS-97 and SHELXL-97 respectively.[12]

Crystal data. $C_{15}H_{27}P_2In$, $M = 384.13$, triclinic, $P\bar{1}$ (no. 2), $a = 6.144(4)$, $b = 1.233(6)$, $c = 13.461(7)$ Å, $\alpha = 112.48(4)$, $\beta = 93.13(5)$, $\gamma = 90.09(5)°$, $V = 856.8(8)$ Å^3, $Z = 4$, $T = 173(2)$ K, $\mu = 3.10$ mm^{-1}, reflections collected 3022, independent reflections 3022, R ($I > 2\sigma I$) = 0.068, $R_w = 0.173$.

CCDC reference number 186/1931.

See http://www.rsc.org/suppdata/dt/b0/b001793k/ for crystallographic files in .cif format.

Computational methods

Calculations performed using density functional methods of the Amsterdam Density Functional Package (version 2.3)[13,14] employed type IV basis sets with triple ξ accuracy sets of Slater type orbitals, with a single polarisation function added; 2p on H, 3d on C, 4d on P and 5d on In. The cores of the atoms were frozen up to 4p for In, 1s for C, 2p for P and treated relativistically using the "Dirac" utility. The generalised gradient approximation (GGA non-local) method was employed, using Vosko, Wilk and Nusair's[15] local exchange correlation with non-local exchange corrections by Becke,[16] non local correlation corrections by Perdew.[17] The valence calculations were quasi-relativistic using the Pauli formalism. The calculations using the Gaussian98[18] program utilized Becke's[19] one parameter hybrid functional method, which includes the non local correlation fuctional of Lee, Yang and Parr[20] together with Vosko, Wilk and Nusair's local exchange correlation, namely BLYP. The calculations employed LanL2DZ basis sets[21] residing in the Gaussian program. This method was also employed for the inner layer of the ONIOM[22] layer developed by Morokuma and co-workers. The outer layer used UFF molecular mechanics method.[23]

Ionisation energies (IE) were determined by means of calculations of the energy of the molecular ions in ground and appropriate excited configurations. The geometry of the ion was taken as the optimised structure of the molecule in order to obtain vertical IE by subtraction of the molecular energy.

Photoelectron spectroscopy

He I and He II photoelectron spectra of **1** and **2** were recorded using a PES Laboratories Ltd. 0078 spectrometer interfaced with an Atari microprocessor. The spectra were calibrated using He, Xe and N_2.

Results and discussion

Structural studies

The molecular structure of **2**, determined by a single crystal X-ray diffraction study, is shown in Fig. 1 with selected bond distances and angles listed in Table 1. The $P_2C_3Bu^t_3$ ring is planar and η^5-ligated to the indium centre. The compound is monomeric, in contrast to the related triphospholyl compound, [In(η^5-$P_3C_2Bu^t_2$)] **1**, where the half sandwich units are linked into chains by weak interactions between the indium centres and adjacent $P_3C_2Bu^t_2$ rings.[3] This difference is presumably because of the larger steric bulk in [In(η^5-$P_2C_3Bu^t_3$)] which prevents the half sandwich units from approaching sufficiently close to allow significant inter-molecular interactions. The indium–centroid distance in [In(η^5-$P_2C_3Bu^t_3$)] is 2.501(9) Å which is similar to the value of 2.598(9) Å found for [In(η^5-$P_3C_2Bu^t_2$)][3] and metal–centroid distances in cyclopentadienyl indium complexes, *e.g.* 2.609 Å in [In(η^5-$C_5H_4SiMe_3$)][24] and 2.53 Å in [In(η^5-$C_5H_4Bu^t$)].[25]

Initially geometries of the hypothetical parent compounds [In($P_3C_2H_2$)], **I**, and [In($P_2C_3H_3$)], **II**, were optimised, with C_s symmetry, as models for **1** and **2** respectively. Density functional calculations were carried out using both the ADF and the Gaussian packages (details are given in the theoretical methods section). Starting geometries were taken from the crystal structures, and the distances and angles found for the local minima are given in Tables 2 and 3.

Table 1 Bond lengths (Å) and angles (°) observed in [In(η^5-$P_2C_3Bu^t_3$)] **2**

In–P1	2.904(3)	P1–C1	1.802(9)
In–P2	2.912(3)	C1–C2	1.429(11)
In–C1	2.829(9)	C2–P2	1.776(10)
In–C2	2.839(9)	P2–C3	1.730(9)
In–C3	2.811(9)	C3–P1	1.725(9)
In–Centroid	2.501(9)		
P1–C1–C2	114.0(7)	P2–C3–P1	116.3(5)
C1–C2–P2	115.8(7)	C3–P1–C1	97.0(4)
C2–P2–C3	96.9(4)		

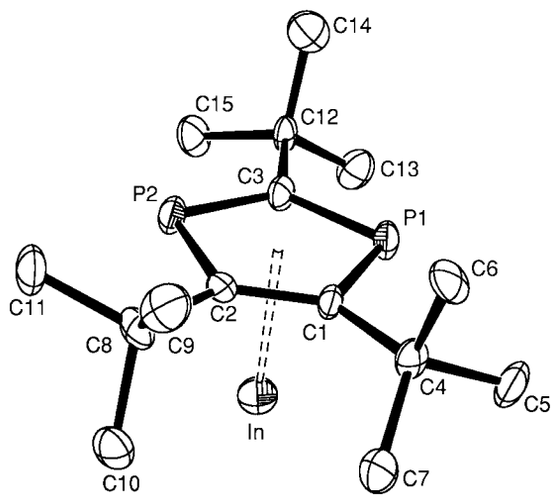

Fig. 1 Molecular structure of **2**, [In(η^5-$P_2C_3Bu^t_3$)].

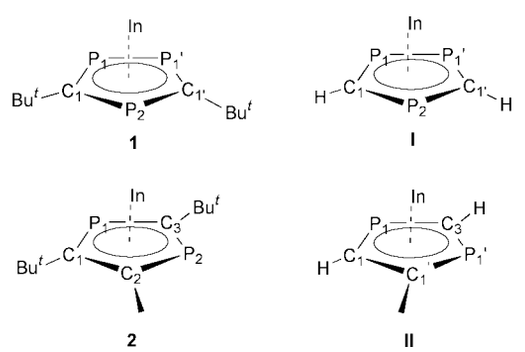

As can be seen from Tables 2 and 3, the ADF calculations tend to underestimate distances while the Gaussian calculations generally slightly overestimate the bond lengths. However, both give a good representation of the structure in spite of the absence in the model of the *tert*-butyl substituents. In terms of angle predictions both calculations underestimate the angles at P and overestimate those at C.

In order to investigate the effect of the bulky substituents on the structure, the ONIOM method was used to carry out a geometry optimisation of **1** where the In and the ring atoms were treated by density functional methods as previously and the *tert*-butyl groups by molecular mechanics. The results are shown in Tables 2 and 3. Although no systematic improvement in distances could be claimed there was a marked improvement in the prediction of ring angles.

Repeated attempts to locate local minima corresponding to an η^1-structure with the In bound to a ring C were unsuccessful

Table 2 Comparison between optimised and experimentally determined structural parameters (distances in Å, angles in °) for **I** and **1**

Method	ADF		G98	ONIOM
	Observed	Calculated	Calculated	Calculated
$In–P_1$	3.035	2.90	3.19	3.21
$In–P_2$	3.108	2.94	3.10	3.08
$In–C_1$	2.981	2.77	2.93	2.92
$P_1–C_1$	1.748	1.75	1.80	1.83
$P_1–P_{1'}$	2.111	2.15	2.34	2.28
$P_2–C_1$	1.781	1.76	1.82	1.85
$C_1–P_1–P_{1'}$	100.2	98	96	98
$P_1–C_1–P_2$	119.8	124	126	121
$C_1–P_2–C_{1'}$	100	96	96	99

Table 3 Comparison between optimised and experimentally determined structural parameters (distances in Å, angles in °) for **II** and **2**

Method	ADF		G98	ONIOM
	Observed	Calculated	Calculated	Calculated
$In–P_1$	2.904/2.912	2.84	3.07	2.97
$In–C_3$	2.811	2.68	2.88	2.86
$In–C_1$	2.829/2.839	2.74	2.85	2.94
$P_1–C_3$	1.730/1.725	1.76	1.82	1.77
$P_1–C_1$	1.802/1.776	1.78	1.85	1.91
$C_1–C_1'$	1.429	1.39	1.41	1.50
$C_1–P_1–C_3$	96.9/97.0	93	92	96
$P_1–C_1–C_1'$	114.0/115.8	117	118	114
$P_1–C_3–P_1'$	116.3	119	120	120

for both **1** and **2**. Such minima were located for In bound to P but lie much higher in energy than the η^5-structures.

Photoelectron spectra of $[In(\eta^5\text{-}P_3C_2Bu^t_2)]$ and $[In(\eta^5\text{-}P_2C_3Bu^t_3)]$

The PE spectra of $[In(\eta^5\text{-}P_3C_2Bu^t_2)]$ and $[In(\eta^5\text{-}P_2C_3Bu^t_3)]$ were recorded with He I (21.21 eV) and He II (40.41 eV) radiation and are shown in Figs. 2 and 3. Important vertical IEs are given in Table 4.

The similarity between the spectra of **1** and **2** is pronounced. Bands **a** and **b** have lower IE for **2** than **1** presumably as a result of the greater number of *tert*-butyl groups in the former. The main band in both spectra, lying between 11 and 17 eV, is predominantly due to ionisation from ring and *tert*-butyl σ orbitals. From previous PE studies on $[In(\eta^5\text{-}C_5H_5)]$, we can anticipate that in the lower IE region, there should be ionisations from two ligand π orbitals and a lone pair orbital associated with the indium atom.[26–28] It is also likely that a σ lone pair orbital for each phosphorus atom resident in the ring will also give bands below 11 eV.

The importance of recording both He I and He II spectra is related to the fact that the photoionization cross-section depends on both the nature of the ionised orbital and the wavelength of the ionising radiation. Comparative analysis of band intensities helps in the assignment of the spectra. A comparison of He I and He II spectra shows that the relative intensity of band **b** increases substantially with increasing photon energy. Indium 5s electrons have a relatively large one electron cross-section at He II excitation levels[29] and therefore band **b** can be readily assigned to an ionisation with significant In 5s character. Band **a** can be assigned to π orbitals which are predominantly ligand in composition. It occurs in an IE region similar to that of C_5H_5 eπ levels. Ionisations from MOs that are highly localized on the phosphorus atoms are expected to show a relative intensity decrease with increasing photon energy. There are no ionisations between 9.5 and 12 eV in the PE spectrum of $[In(\eta^5\text{-}C_5H_5)]$, thus there is no equivalent ionisation to bands **c** and **d** of **1**. From the decrease in relative intensity of these bands from the He I to the He II spectrum we can conclude

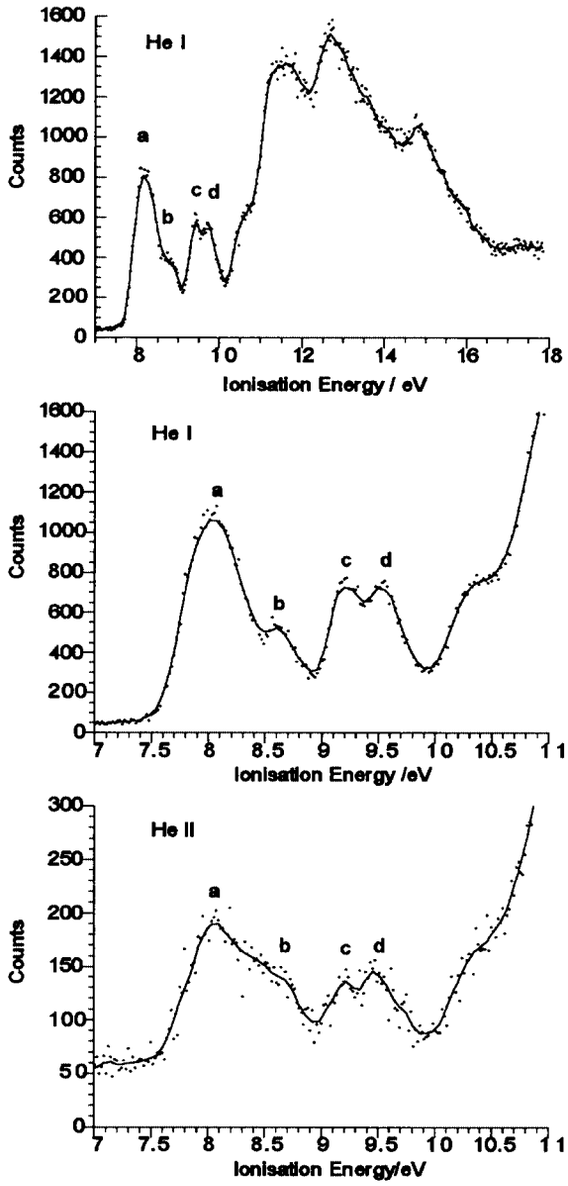

Fig. 2 He I and He II PE spectra of **1**, $[In(\eta^5\text{-}P_3C_2Bu^t_2)]$.

bands **c** and **d** are due to P lone pairs. A similar argument might be applied to bands **c** and **d** of **2** but **d** lies at higher energy in the region normal for *tert*-butyl ionisations and **2** has fewer P atoms than **1** so such an assignment would need confirmation.

Ground-state electronic structure

For **I** and **II** the energies of the highest occupied molecular orbitals and the LUMOs using both ADF and Gaussian are shown in Table 5. The energies are generally 0.3 to 0.5 eV higher in energy for Gaussian than ADF but show similar groupings and orderings except in the case of **I** where the order of the 10a′ and 7a″ is reversed between the two methods. This aspect will be discussed below.

ADF enables a fragment analysis of the electronic structure wherein the composition of a MO is given in terms of the basis orbitals of fragments. In these cases the In and the rings were chosen as the fragments. The results of this analysis are given in Table 6 and are used for the construction of the MO diagrams given in Figs. 4 and 5. Pictorial representations of the MO are given in Figs. 6 and 7.

For both the P_3C_2 and the P_2C_3 rings an out-of-phase combination of P pσ orbitals gives a high lying MO (7a′ and 4a″ respectively) of similar energy to the highest occupied ring π orbitals. Other combinations (4a″ and 6a′ for **I**, and 7a′ for **II**)

Table 4 Vertical IE of [In(η^5-$P_3C_2Bu^t_2$)] and [In(η^5-$P_2C_3Bu^t_3$)], calculated IE for [In(η^5-$P_3C_2H_2$)] and [In(η^5-$P_2C_3H_3$)] and band assignments

	MO	Orbital energy ε_i/eV (ADF)	Calculated IE/eV (ADF)	Orbital type	Experimental IE/eV
I and **1**	12a′	−6.03	8.54	P-σ	
	11a′	−6.23	8.65	Ring π + In	8.1 **a**
	7a″	−6.78	9.24	Ring π + In	
	10a′	−6.69	9.21	In 5s	8.6 **b**
	6a″	−7.43	10.11	P σ	9.3 **c**
	9a′	−7.63	10.28	P σ	9.6 **d**
2 and **II**	7a″	−6.03	8.57	Ring π + In	7.5 $\mathbf{a_1}$
	6a″	−6.31	9.02	P σ	
	12a′	−6.29	9.42	Ring π + In	7.9 $\mathbf{a_2}$
	11a′	−6.88	8.82	In 5s	8.5 **b**
	10a″	−7.77	10.48	P σ	9.4 **c**
	5a″	−8.61	11.43	Bu^t orbital	9.7 **d**

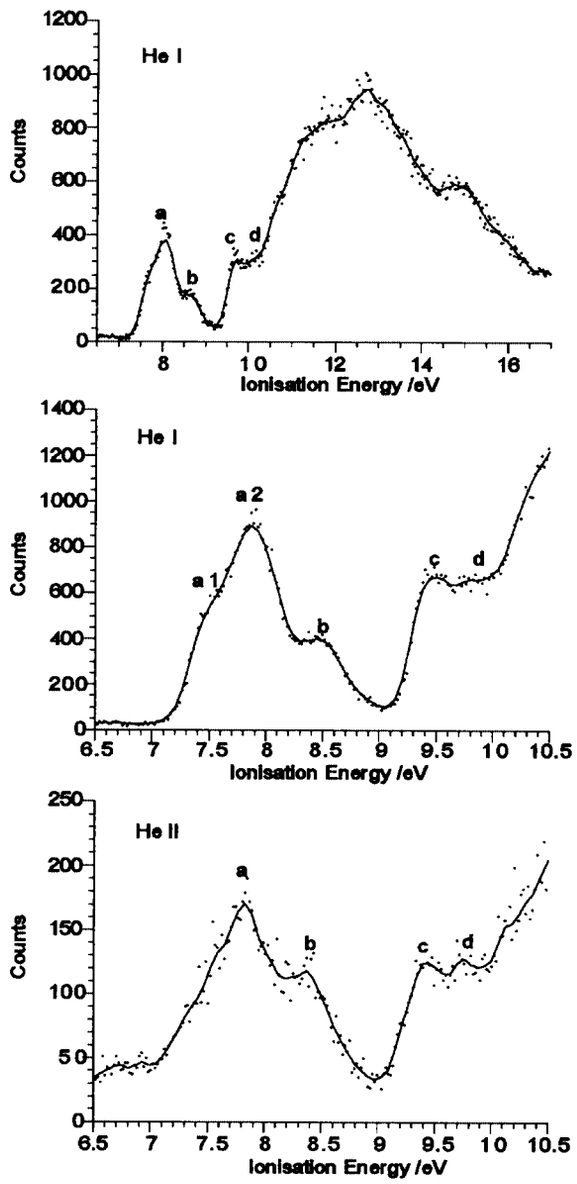

Fig. 3 He I and He II PE spectra of **2**, [In(η^5-$P_2C_3Bu^t_3$)].

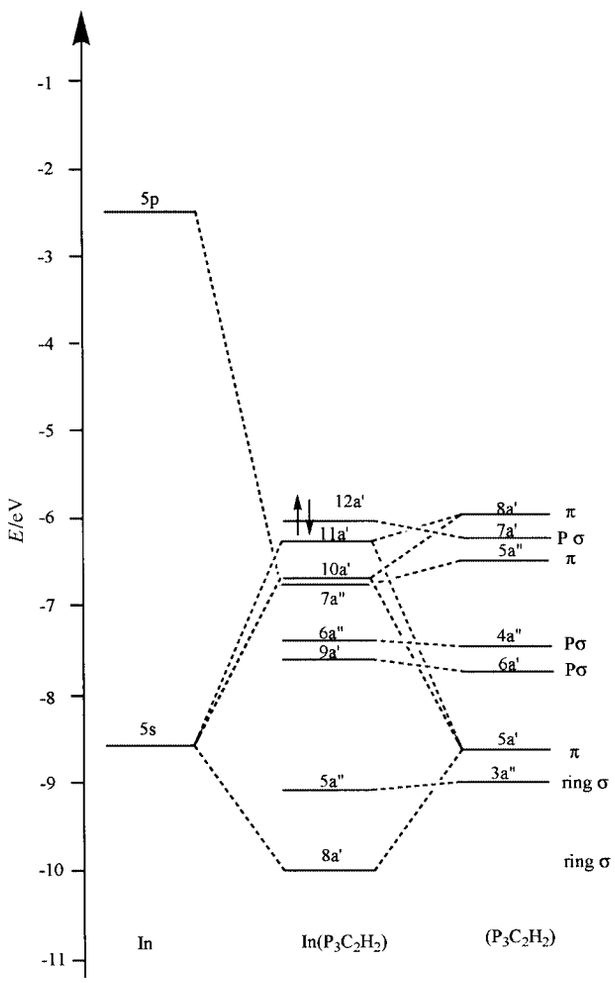

Fig. 4 MO diagram for **I**, [In(η^5-$P_3C_2H_2$)].

lie over 1 eV lower in energy yet above the most stable ring π orbital. The corresponding Pσ orbitals in **I** and **II** lie at very similar energies to the ring fragment orbitals and mix very little with the In orbitals (Table 6). Some mixing with fragment π orbitals on complex formation indicates a small rehybridisation at the P atoms which may well improve overlap with the In.

In both **I** and **II** the composition of the 7a″ MO shows that the upper π orbitals of a″ symmetry mix to a small amount with the appropriate In 5p orbital. The principal mixing is within the a′ set of orbitals. The In 5s orbital lies very close in energy to the lowest ligand π orbital and mixes with this strongly, with both the bonding and antibonding combinations being occupied. The resulting anti-bonding combination lies close in energy to the upper π orbitals and further mixing ensues. Consequently In 5s character is spread across the 8a′, 11a′ and 12a′ orbitals for **II**. For **I** the bonding combination mixes further with a close lying ring σ orbital and the 7a′, 8a′, 10a′ and 11a′ orbitals all possess significant In 5s character. This delocalisation of In 5s character is apparently at odds with the PE spectrum where band **b** can be clearly identified with an

Table 5 Orbital energies (eV) for optimised structures of **I** and **II** using both ADF and Gaussian and orbital energies for **1** and **2** from a single point Gaussian calculation using optimised structures from the ONIOM method

MO	**I** ADF	**I** Gaussian	**1** Gaussian	Type
8a″ (LUMO)	−2.57	−2.36		
12a′ (HOMO)	−6.02	−5.60	−5.05	P σ
11a′	−6.22	−5.79	−5.39	Ring π + In
10a′	−6.68	−6.50	−5.95	In s + ring π
7a″	−6.77	−6.27	−5.49	Ring π + In p
6a″	−7.42	−7.24	−6.45	P σ
9a′	−7.63	−7.26	−6.62	P σ
8a′	−10.10	−9.34	−7.50	Ring π + In s
MO	**II** ADF	**II** Gaussian	**2** Gaussian	Type
13a′ (LUMO)	−2.03	−1.75	−1.16	
7a″ (HOMO)	−6.04	−5.51	−4.85	Ring π + In p
12a′	−6.29	−5.97	−4.98	Ring π + In s
6a″	−6.31	−6.01	−5.01	P σ
11a′	−6.88	−6.40	−5.64	In s + ring π
10a′	−7.76	−7.37	−6.45	P σ
5a″	−8.61	−8.24	−6.64	Ligand σ
8a′	−10.28	−9.32	−7.21	Ring π + In s

Table 6 Fragment analyses of [In(η^5-$P_3C_2H_2$)] and [In(η^5-$P_2C_3H_3$)]

	% In		% ($P_3C_2H_2$)						
I MO	5s	5p	Ring σ	5a′ π	6a′ Pσ	4a″ Pσ	5a″ π	7a′ Pσ	8a′ π
12a′								86	11
11a′	14	7		6				12	58
10a′	45	5		28					19
7a″		8					90		
6a″						99			
9a′					99				
5a″			99						
8a′	26		26	44					
7a′	9		73	14					
	% In		% ($P_2C_3H_3$)						
II MO	5s	5p	Ring σ	6a′ π	ring σ	7a′ Pσ	4a″ Pσ	8a′ π	5a″ π
7a″		11							86
12a′	39			14				38	
6a″							99		
11a′	25	4		15				53	
10a′						99			
5a″					100				
9a′									
8a′	32			63					

In s based ionisation. However, the population analysis shows (Table 6) that out of these four orbitals the 10a′ orbital has the highest In 5s content.

As noted above the Gaussian calculation on **I** gives a different ordering of the 10a′ orbital, placing it lower in energy, and inspection of the isosurface (Fig. 8) shows it to have a more lone pair like appearance than the corresponding ADF orbital (Fig. 6). There is therefore a more direct relationship between the Gaussian orbital manifold and the PE spectrum than is found for the ADF calculation. The same is found for the Gaussian calculation of **II** (Fig. 8).

Consideration of the gross population of the fragment orbitals and the Mulliken charges listed in Table 7, shows that charge transfer from the indium to the ring occurs by depopulation of the In 5p orbital and occupation of the ring 5a″ and 8a′ π orbitals.

Calculation of ionisation energies

IEs were estimated as the difference between the molecular ground state energy and the ion energy in the ground or an excited state. ADF enables the calculation of ion states using as a basis set the MO of the uncharged molecule. This not only assists convergence but also enables analysis of the "hole" in the molecular ion in terms of the MO of the molecule.

Calculated IEs for **I** and **II** are given in Table 4. Good agreement with the values from the spectra of **1** and **2**, and the initial band assignments suggests that band **a** in both cases comprises ionizations from the upper π orbitals of the ring and a high lying Pσ orbital. In the case of **1** bands **c** and **d** are both attributed to Pσ ionizations as deduced above, but in the case of **2** only band **c** may be given such an assignment. For **1**, there is a reversal of ordering between the 7a″ and 10a′ orbitals and the 7A″ and 10A′ IE bands.

As both **1** and **2** contain *tert*-butyl groups (which are replaced with H atoms in the calculations) the ionisation energies should be shifted to lower energies in the experimental compound by comparison with the calculated version. Using the optimised geometry from the ONIOM calculations and performing a

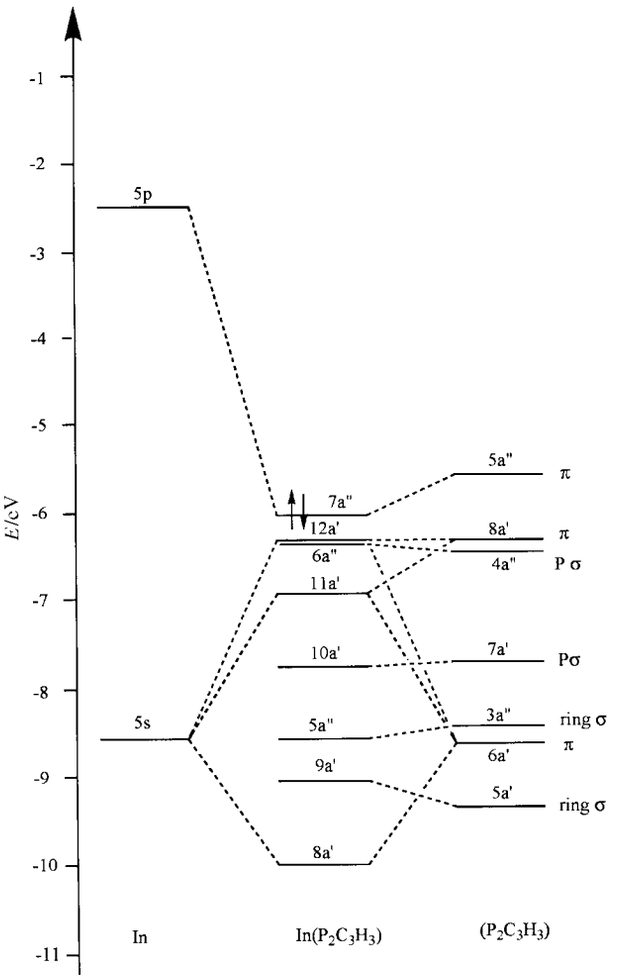

Fig. 5 MO diagram for **II**, [In(η^5-$P_2C_3H_3$)].

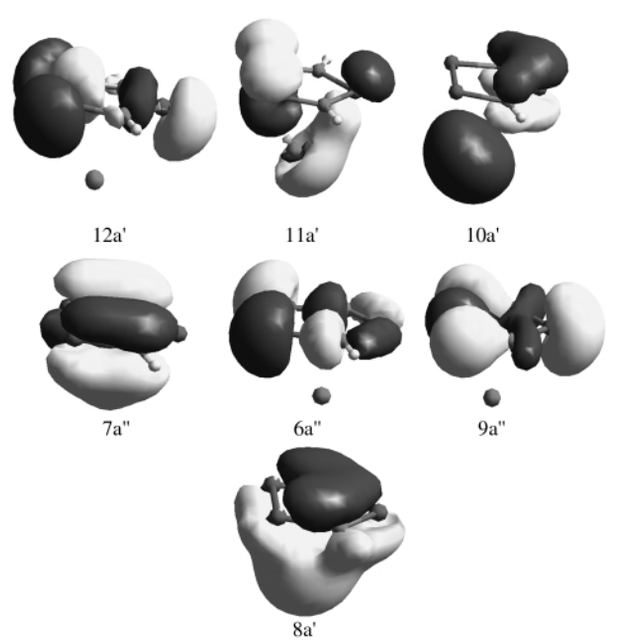

Fig. 6 Highest occupied orbitals of **I**, [In(η^5-$P_3C_2H_2$)].

single point energy calculation on the whole molecule gave orbital energies that were higher than the orbital energies when the *tert*-butyl groups were not included (Table 5). The difference ranged from 0.4 to 0.6 eV for **1/I** and from 0.7 to 1 eV for **2/II**. Taking this factor into account, the calculated ionisation energies would be expected to be lowered by a similar amount giving closer agreement with experiment.

Table 7 Gross population of fragment orbitals and Mulliken charges on In, C and P atoms for **I** and **II**

Gross populations

	In		Ring						
FO	5s	5p	5a′	6a′	3a″	7a′	4a′	8a′	5a″
I	1.97	0.58	1.87	2	2	1.99	2	1.75	1.82
II	1.99	0.50	2	1.86	2	2	2	1.83	1.74

Mulliken charges

	In	C1	C2	P1	P2
I	0.38	0.33		−0.24	−0.34
II	0.38	0.22	0.31	−0.37	

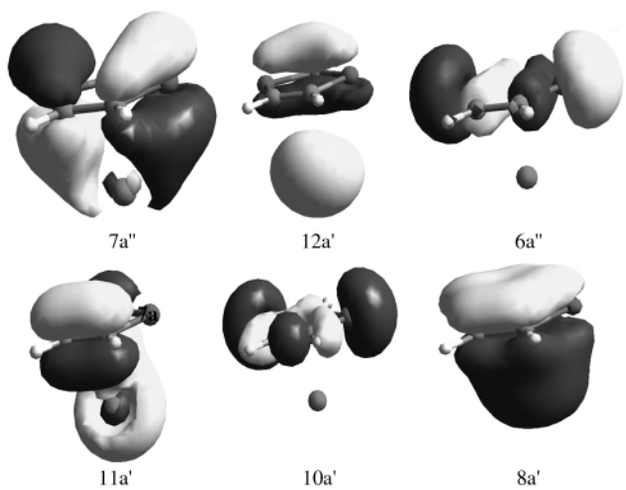

Fig. 7 Highest occupied orbitals of **II**, [In(η^5-$P_2C_3H_3$)].

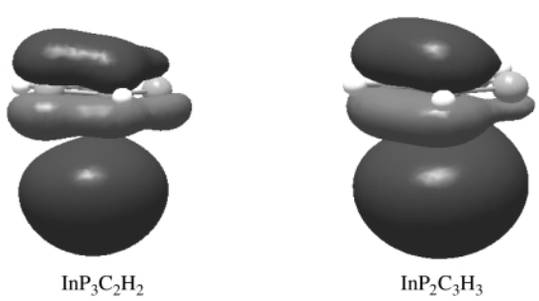

Fig. 8 Isosurface for the 10a′ orbital of **I** and 11a′ orbital of **II** from the Gaussian calculations.

Comparison with [In(η^5-C_5H_5)]

The gas phase structure of [In(η^5-C_5H_5)] has been shown by electron diffraction to have the cyclopentadienyl ring coordinated in a η^5-fashion.[6,7] The bonding in cyclopentadienylindium is summarized in a paper by Eisenstein and Canadell.[28]

Full geometry optimisation was performed on [In(η^5-C_5H_5)] starting with a half sandwich geometry with C_{5v} symmetry. The comparison between calculated structural parameters and experimental parameters (Table 8) is very satisfactory. Calculated IE values agree well with the results of PES studies of [In(η^5-C_5H_5)] recorded by Egdell *et al.*[27] Two PE bands were observed in the low IE regions of the spectra. The first band is assigned to the e_1 (π) MOs of the hydrocarbon ring, on the basis of the unchanging nature of the peak between the spectra of indium cyclopentadienyl and the thallium analogue. The first ionisation energy in [In(η^5-C_5H_5)] is 8.28 eV (Table 9), which is slightly higher than the first band of **1** (8.1 eV). This leads to the

Table 8 Comparison of calculated and experimental structural parameters for [In(η^5-C_5H_5)]

	Distances/Å	
	Observed	Calculated
C–C	1.43	1.41
C–In	2.62	2.61
Cen–In	2.32	2.31

Table 9 Comparison between calculated and experimental IE for [In(η^5-C_5H_5)]

Band	Observed/eV	Calculated/eV	Orbital	Assignment
A	8.28	8.57	$4e_1$	Ligand e_1 (π)
B	9.23	9.22	$5a_1$	a_1 (5s)
C	12.89	12.06	$3e_2$	Ligand σ
		12.39	$3e_1$	Ligand σ
		13.37	$4a_1$	a_1 (π)

Table 10 Fragment analysis of [In(η^5-C_5H_5)]

		In		C_5H_5	
MO	Energy/eV	5s	5p	a_1 π	e π
$4a_1$	−10.49	27		69	
$5a_1$	−6.33	74	6	21	
$4e_1$	−5.81		9		89

conclusion that the presence of the phosphorus atoms almost cancels the effect of the *tert*-butyl groups, which would be expected to move the ionisation energies to significantly lower values. The fragment analysis (Table 10) shows that the π orbitals in **I** and **II** (7a″ and 11a′) show slightly more mixing between the ligand and indium than the HOMO in [In(η^5-C_5H_5)].

The second band is assigned to the ionisation of the 5s (a_1) electrons on indium (the In "lone pair") due to the relative increase in intensity of the peak recorded in the He II spectra. The ionisation energy of the lone pair is higher in [In(η-C_5H_5)] than in **1** and **2**. Population analysis (Table 10) shows that it has greater In 5s character. The higher IE bands were assigned to electrons associated with the "σ framework" of the C_5H_5 ring and the ring π_1 orbital.

Conclusions

Both the structures and the PE spectra of [In(η^5-$P_3C_2Bu^t_2$)] and [In(η^5-$P_2C_3Bu^t_3$)] are well modelled by density functional calculations on [In(η^5-$P_3C_2H_2$)] and [In(η^5-$P_2C_3H_3$)]. The orbital ordering places a high lying Pσ orbital close in energy to the two top occupied ring π levels which mix with the In $5p_x$ and $5p_y$ orbitals. This Pσ orbital is antibonding across the ring and an In ring antibonding orbital with In 5s character lies below these. Other electrons in Pσ are more tightly bound. A ring π In 5s bonding orbital has similar energy to the ring σ bonding orbitals. Comparison with [In(η^5-C_5H_5)] shows the bonding in the two compounds to be very similar.

Acknowledgements

We thank the EPSRC for post-doctoral support (for GKBC and MDF). Part of this work has been carried out using computational resources of a DEC 8400 multiprocessor cluster (Columbus/Magellan), provided by the U.K. Computational Chemistry Facility at Rutherford Appleton Laboratory.

References

1 C. Dohmeier, D. Loos and H. Schnockel, *Angew. Chem., Int. Ed. Engl.*, 1996, **108**, 141.
2 A. Schnepf, G. Strober, D. Carmichael, F. Mathey and H. Schnockel, *Angew. Chem., Int. Ed.*, 1999, **38**, 1646.
3 C. Callaghan, G. K. B. Clentsmith, F. G. N. Cloke, P. B. Hitchcock, J. F. Nixon and D. M. Vickers, *Organometallics*, 1999, **18**, 793.
4 E. O. Fischer and H. P. Hoffmann, *Angew. Chem.*, 1957, **69**, 639.
5 E. O. Fischer, *Angew. Chem.*, 1957, **69**, 207.
6 E. Frasson, F. Menegus and C. Panattoni, *Nature* (*London*), 1963, **199**, 1087.
7 A. Haaland, *Top. Curr. Chem.*, 1975, **53**, 1.
8 J. F. Nixon, *Coord. Chem. Rev.*, 1995, **145**, 201 and references therein; K. B. Dillon, F. Mathey and J. F. Nixon, *Phosphorus: The Carbon Copy*, John Wiley and Sons, New York, 1998, p. 366 and references therein.
9 J. J. Durkin, M. D. Francis, P. B. Hitchcock, C. Jones and J. F. Nixon, *J. Chem. Soc., Dalton Trans.*, 1999, 4057.
10 T. Douglas, K. H. Leopold, A. L. Haggerty and A. Rheingold, *Polyhedron*, 1990, **9**, 329.
11 D. Carmichael, L. Ricard and F. Mathey, *J. Chem. Soc., Chem. Commun.*, 1994, 1167.
12 G. M. Sheldrick, SHELXS-97, SHELXL-97, University of Göttingen, 1997.
13 G. te Velde and E. J. Baerends, *J. Comput. Phys.*, 1992, **99**, 84.
14 E. J. Baerends, E. G. Ellis and P. Ros, *Chem. Phys.*, 1973, **2**, 41.
15 S. H. Vosko, L. Wilk and M. Nusair, *Can. J. Phys*, 1990, **58**, 1200.
16 A. D. Becke, *Phys. Rev. A*, 1988, **38**, 2398.
17 J. Perdew, *Phys. Rev. B*, 1986, **33**, 8822.
18 Gaussian98, M. J. Frisch, G. W. Trucks, B. H. Schlegel, G. E. Scuseria, M. A. Robb, J. R. Cheeseman, V. G. Zakrzewski, J. A. Montgomery, R. E. Stratmann, J. C. Burant, S. Dapprich, J. M. Millam, A. D. Daniels, K. N. Kundin, M. C. Strain, O. Faraks, J. Tomaski, V. Barone, M. Cossi, R. Cammi, C. Mennucci, C. Pomelli, C. Adamo, S. Clifford, J. Ochterski, G. A. Petersson, P. Y. Ayala, Q. Cui, K. Morokuma, D. K. Malick, A. D. Rabuck, K. Raghavachari, J. B. Foresman, R. Gomperts, R. L. Martin, D. J. Fox, T. Keith, M. A. Al-Laham, C. Y. Peng, A. Nanayakkara, C. Gonzalez, M. Challacombe, P. M. W. Gill, B. G. Johnson, W. Chen, M. W. Wong, J. L. Andres, M. Head-Gordon, E. S. Replogle and J. A. Pople, Gaussian Inc., Pittsburgh, PA, 1998.
19 A. D. Becke, *J. Chem. Phys.*, 1996, **104**, 1040.
20 C. Lee, W. Yang and R. G. Parr, *Phys. Rev. B*, 1988, **37**, 785.
21 P. J. Hay and W. R. Wadt, *J. Chem. Phys.*, 1985, **82**, 299.
22 S. Dapprich, I. Komaromini, K. S. Byun, K. Morokuma and M. J. Frisch, *Theochem. J. Mol. Struct.*, 1999, **462**, 1.
23 A. K. Rappe, C. J. Casewit, K. S. Colwell, W. A. Goddard III and W. M. Skiff, *J. Am. Chem. Soc.*, 1992, **114**, 10024.
24 O. T. Beachley, J. F. Lees, T. E. Glassman, M. R. Churchill and L. A. Buttrey, *Organometallics*, 1990, **9**, 2488.
25 O. T. Beachley, J. F. Lees and R. D. Rogers, *J. Organomet. Chem.*, 1991, **418**, 165.
26 S. Cradock and W. Duncan, *J. Chem Soc., Faraday Trans. 2*, 1978, **74**, 194.
27 R. G. Egdell, I. Fragala and A. F. Orchard, *J. Electron Spectrosc. Relat. Phenom.*, 1978, **14**, 467.
28 O. Eisenstein and E. Canadell, *Organometallics*, 1984, 759.
29 J. J. Yeh, *Atomic and Nuclear Data Tables*, AT & T, Gordon Breach, Langhorne, 1993.